Catalytic Mechanism of Scytalone Dehydratase: Site-Directed Mutagenisis, Kinetic Isotope Effects, and Alternate Substrates

Gregory S. Basarab,[‡] James J. Steffens,[‡] Zdzislaw Wawrzak,[§,||] Rand S. Schwartz,[‡] Tomas Lundqvist,[⊥] and Douglas B. Jordan*[,‡]

E. I. DuPont de Nemours Agricultural Products, Stine-Haskell Research Center, P.O. Box 30, Newark, Delaware 19714, E. I. DuPont de Nemours Life Sciences, Experimental Station, Wilmington Delaware 19880-0228, and Astra Structural Chemistry Laboratory, S-431 83, Mölndal, Sweden

Received December 16, 1998; Revised Manuscript Received March 5, 1999

ABSTRACT: On the basis of the X-ray crystal structure of scytalone dehydratase complexed with an active center inhibitor [Lundqvist, T., Rice, J., Hodge, C. N., Basarab, G. S., Pierce, J. and Lindqvist, Y. (1994) *Structure (London) 2*, 937−944], eight active-site residues were mutated to examine their roles in the catalytic mechanism. All but one residue (Lys73, a potential base in an anti elimination mechanism) were found to be important to catalysis or substrate binding. Steady-state kinetic parameters for the mutants support the native roles for the residues (Asn131, Asp31, His85, His110, Ser129, Tyr30, and Tyr50) within a syn elimination mechanism. Relative substrate specificities for the two physiological substrates, scytalone and veremelone, versus a Ser129 mutant help assign the orientation of the substrates within the active site. His85Asn was the most damaging mutation to catalysis consistent with its native roles as a general base and a general acid in a syn elimination. The additive effect of Tyr30Phe and Tyr50Phe mutations in the double mutant is consistent with their roles in protonating the substrate's carbonyl through a water molecule. Studies on a synthetic substrate, which has an anomeric carbon atom which can better stabilize a carbocation than the physiological substrate (vermelone), suggest that His110Asn prefers this substrate over vermelone in order to balance the mutation-imposed weakness in promoting the elimination of hydroxide from substrates. All mutant enzymes bound a potent active-site inhibitor in near 1:1 stoichiometry, thereby supporting their active-site integrity. An X-ray crystal structure of the Tyr50Phe mutant indicated that both active-site waters were retained, likely accounting for its residual catalytic activity. Steady-state kinetic parameters with deuterated scytalone gave kinetic isotope effects of 2.7 on k_{cat} and 4.2 on k_{cat}/K_m, suggesting that steps after dehydration partially limit k_{cat}. Pre-steady-state measurements of a single-enzyme turnover with scytalone gave a rate that was 6-fold larger than k_{cat}. k_{cat}/K_m with scytalone has a pK_a of 7.9 similar to the pK_a value for the ionization of the substrate's C6 phenolic hydroxyl, whereas k_{cat} was unaffected by pH, indicating that the anionic form of scytalone does not bind well to enzyme. With an alternate substrate having a pK_a above 11, k_{cat}/K_m had a pK_a of 9.3 likely due to the ionization of Tyr50. The non-enzyme-catalyzed rate of dehydration of scytalone was nearly a billion-fold slower than the enzyme-catalyzed rate at pH 7.0 and 25 °C. The non-enzyme-catalyzed rate of dehydration of scytalone had a deuterium kinetic isotope effect of 1.2 at pH 7.0 and 25 °C, and scytalone incorporated deuterium from D_2O in the C2 position about 70-fold more rapidly than the dehydration rate. Thus, scytalone dehydrates through an E1cb mechanism off the enzyme.

Scytalone dehydratase (SD, EC 4.2.1.94)[1] catalyzes the dehydrations of scytalone and vermelone in the fungal melanin biosynthetic pathway (Figure 1). The pathogenic competence of *Magnaporthe grisea* is normally dependent on the ability of the fungus to synthesize fungal melanin during the infection process (*1*−*3*). *M. grisea* is a filamentous ascomycete responsible for the economically significant disease known as rice blast, which occurs nearly everywhere in the world where rice is grown extensively (*4*). As part of a target-site design program to discover rice blast fungicides, we began to characterize enzymes involved in the biosynthesis of 1,8-dihydroxynaphthalene, the precursor of fungal melanin. The X-ray crystal structures of *M. grisea* SD (*5*) and 3HN reductase (*6*), two enzymes from the pathway which are the targets of commercial fungicides, are the first three-dimensional structures determined for fungicide-targeted enzymes from an agronomically important pathogen. Potent inhibitors of the enzymes have been designed and characterized (*7*, *8*).

There are three mechanisms that must be considered for the dehydration of scytalone (Scheme 1). An E1cb mechanism evokes a rapid reversible enolate formation followed by a slow loss of hydroxide. Discrete enolate formation is unlikely at physiological pH nor is there an enzymic base

* To whom correspondence should be addressed. Address: Stine-Haskell Research Center, Building 300, Elkton Road, P.O. Box 30, Newark, DE 19714. Tel: (302) 451-0075. Fax: (302) 366-5738. E-mail: doug.b.jordan@usa.dupont.com.

[‡] E. I. DuPont de Nemours Agricultural Products.

[§] E. I. DuPont de Nemours Life Sciences.

[||] Present address: Northwestern University, DND-CAT Bldg. 432/A001, 9700 S. Cass Ave., Argonne, IL 60439.

[⊥] Astra Structural Chemistry Laboratory.

10.1021/bi982952b CCC: $18.00
Published on Web 04/21/1999

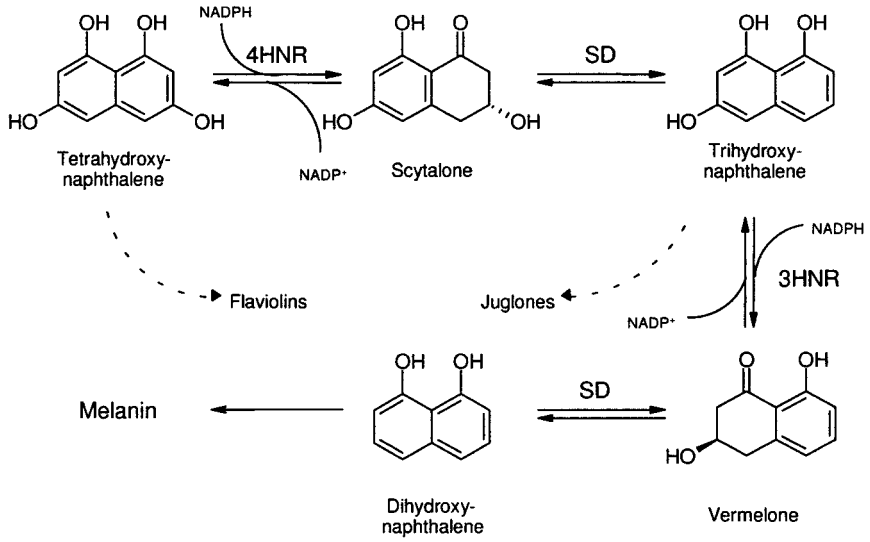

FIGURE 1: The fungal melanin biosynthetic pathway: 4HNR = tetrahydroxynaphthalene reductase; SD = scytalone dehydratase; 3HNR = trihydroxynaphthalene reductase.

Scheme 1: Potential Mechanisms for the Dehydration of Scytalone

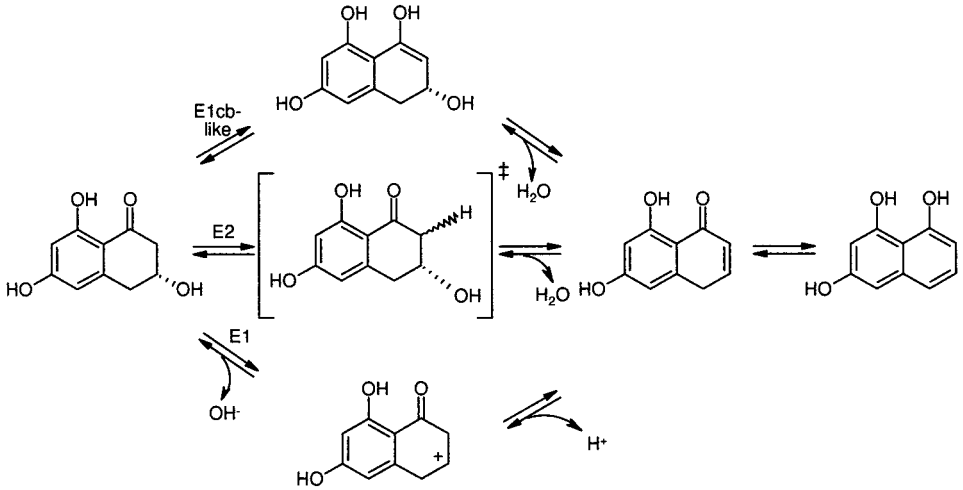

strong enough to effect such a transformation (*9*−*11*). Rather an E1cb-like mechanism would invoke protonation of the substrate's carbonyl, promoting the removal of the α-hydrogen atom to form an enol intermediate. Gerlt and Gassman refer to this mechanism as a concerted general acid/base-catalyzed enolization followed by vinylogous E2 elimination (*10*). An E2 mechanism involves a concerted removal of the α-hydrogen atom with the loss of hydroxide. An E1 elimination entails a rapid loss of hydroxide to leave a carbocation intermediate before slow deprotonation. It should be recognized that there is a continuum of possible mechanisms in going from an E1cb to an E1, in which the relative timing of α-deprotonation and hydroxide loss lies between the two extremes (*12*).

An interesting feature that provides some experimental accessibility to the catalytic mechanism of SD is that nearly all of the contacts with active-site inhibitors are made with the side chains of enzymic residues. The contacts with substrate scytalone are predicted to occur exclusively with enzymic side chains. The absolute stereochemistries of SD's natural substrates, scytalone and vermelone, are known (*13*). Two conformations of scytalone are considered favorable for the dehydration reaction, both of which orient the C3 hydroxyl axially (see Figure 2 for scytalone numbering). One conformation can be described as a boat having a syn-diaxial orientation between the C2 hydrogen and the hydroxyl; the other, as an envelope with a corresponding anti-diaxial orientation.[2] The two conformations for scytalone were mapped onto the structure of salicylamide inhibitor **1** (Figure 3) within the original X-ray model (1STD) (*5*) of the SD active site for visualization.

[1] Abbreviations: SD, scytalone dehydratase; KIE, kinetic isotope effect; DDBO, 2,3-dihydro-2,5-dihydroxy-4H-benzopyran-4-one; HBO, 5-hydroxy-4*H*-benzopyran-4-one; DMSO, dimethyl sulfoxide; EIMS, electrospray ionization mass spectrometry; SDS, sodium dodecyl sulfate; SDS−PAGE, sodium dodecyl sulfate−polyacrylamide gel electrophoresis; 1STD, the PDB accession code for the original X-ray structure of scytalone dehydratase; DHS, *des*-hydroxyscytalone or 3,4-dihydro-6,8-dihydroxy-1(2H)-naphthalenone; ^{13}C-DHS, ^{13}C-labeled *des*-hydroxyscytalone or 3,4-dihydro-6,8-dihydroxy-1(2H)-2-^{13}C-naphthalenone; k_{non}, the rate of the reaction in the absence of enzyme; 3HN, 1,3,8-trihydroxynaphthalene; 4HN, 1,3,6,8-tetrahydoxynaphthalene; DBO, 4,5-dihydroxy-2H-benzopyran-2-one; PCR, polymerase chain reaction; D_6-scytalone, 2,2,4,4,5,7-hexadeuterioscytalone; DTT, dithiothreitol; Mes, 2[*N*-morpholino]ethanesulfonic acid; Tris, tris(hydroxymethyl)aminomethane; Hepes, *N*-[2-hydroxyethyl]piperazine-*N*′-[2-ethanesulfonic acid]; Mops, 3-[*N*-morpholino]propanesulfonic acid; Ampso, 3-[(1,1-dimethyl-2-hydroxyethyl)amino]-2-hydroxy-propanesulfonic acid; Capso, 3-[cyclohexylamino]-2-hydroxy-1-propanesulfonic acid; E1, elimination first-order; E1cb, elimination first-order conjugate base; E2, elimination second-order (concerted).

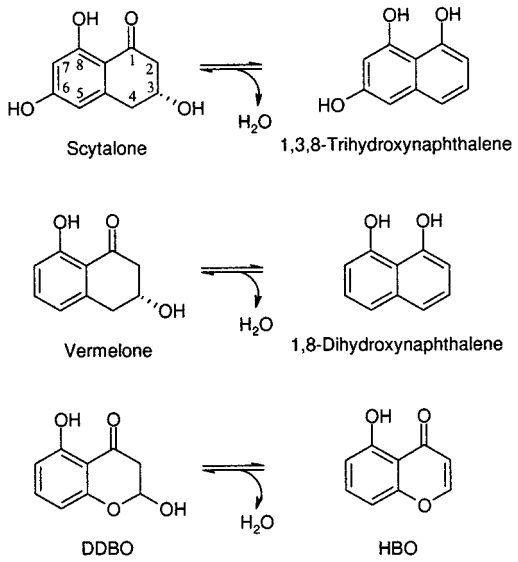

FIGURE 2: Reactions catalyzed by scytalone dehydratase.

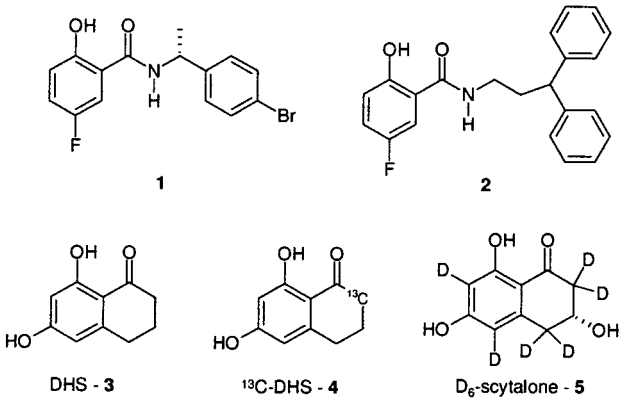

FIGURE 3: Molecules discussed in this work.

In Figure 4A, scytalone is poised in the active site for a syn-diaxial elimination. The imidazole of H85 is in a good position to remove the axially disposed C2 proton of substrate and then donate the proton to the C3 hydroxyl leaving group. The basicity of the H85 imidazole could be enhanced through a hydrogen bond with the carboxyl group of D31. The hydroxyl groups of Y30 and Y50 could increase the acidity of the associated water molecule for hydrogen bonding to the substrate's carbonyl. Acid catalysis by the two tyrosine residues in concert with a bound water molecule has been shown by molecular orbital theory to stabilize enol formation in a proposed transition state for the dehydration (*14*). H110 could assist in stretching the bond of the C3 hydroxyl leaving group. The ND2 atom of the N131 amide could help protonate the substrate's carbonyl to induce enol formation in a relay through donation of a hydrogen to the substrate's C8 phenolic hydroxyl, and the amide functionality could serve for substrate recognition in productive binding. S129 is positioned to form a hydrogen bond with the C6 hydroxyl of scytalone for substrate recognition. In a recent review on β-elimination mechanisms, Anderson suggests a syn elimination mechanism for the enzyme-catalyzed dehydration of scytalone (*12*).

In Figure 4B, scytalone is poised in the active site for a anti-diaxial elimination. Potential roles for the amino acid side chains remain the same as with the syn-diaxial elimination mechanism with the exception of H85, which is not well-positioned to abstract the Cα proton. In this model, H85 would be protonated (interaction with the carboxyl group of D31 would elevate its pK_a) for neutralization of the substrate's hydroxyl leaving group. There is no available enzymic base to remove the axial C2 proton from the substrate. It was suggested from inspection of the initial X-ray structure (1STD) that SD undergoes a structural reorganization on binding inhibitor **1** due to the bulky bromophenyl group thought to disrupt an α-helix flanking K73, thereby displacing the residue from the active site (*5*). Restoring the region around K73 to a helix would bring the residue into a position to participate as a catalytic base. K73 which extends into solvent as given by the X-ray structure thus became a candidate for mutational analysis to support or eliminate this hypothesis. As well, the other seven above-mentioned residues were mutated in this work to examine their roles in the catalytic mechanism.

An alternative hypothesis might have SD catalyzing the dehydration by removal of an axial proton from C4 which could be activated through conjugation in the scytalone aromatic ring to the carbonyl functionality. Though not in an ideal orientation, H110 lies about 4 Å from this proton in our model. However, in addition to catalyzing the dehydrations of physiological substrates scytalone and vermelone, SD efficiently catalyzes the dehydration of a nonphysiological substrate (DDBO, Figure 2) (*15*). In our model, DDBO displays an oxygen atom toward H110 rather than the C4 methylene of scytalone. Since DDBO is a better substrate than scytalone for the enzyme-catalyzed dehydration, H110 does not likely function as a base for removing a proton from C4 of scytalone. The function of H110 is examined in this work through changes to alanine and asparagine.

Relative substrate specificity measurements comparing DDBO and scytalone suggested that the enzyme may have an early transition state with respect to the hydroxide leaving group of DDBO (*15*). This suggestion is re-examined in this work through pre-steady-state rate measurements and studies with the alternate physiological substrate vermelone. Also, we synthesized ^{13}C-labeled *des*-hydroxyscytalone (^{13}C-DHS; Figure 3) to determine if we could detect favorable binding of the enol form of the substrate. In the same vein, we investigated the SD-catalyzed dehydration of scytalone in D_2O to determine if a reversible enol formation could be trapped during catalysis, thus examining an E1cb-like mechanism as reported for some enzyme-catalyzed reactions (*12*). Additional studies relevant to the mechanism of the SD-catalyzed reactions are reported: the kinetic isotope effect for deuterated scytalone in the enzyme-catalyzed and in the solvolytic, non-enzyme-catalyzed dehydration reactions, and the pH dependencies of the enzyme's kinetic parameters for scytalone and DDBO.

[2] Clearly, the C2 hydrogen and the C3 hydroxyl need to be in the axial orientation for removal, but not necessarily simultaneously. For example, a second envelope conformation of scytalone orients the C3 hydroxyl equatorially and a C2 hydrogen axially. The axial hydrogen could be removed prior to a conformational change of the enol intermediate to orient the C3 hydroxyl axially for elimination. The two diaxial conformations of scytalone serve to illustrate the syn and anti elimination mechanisms in a simple fashion.

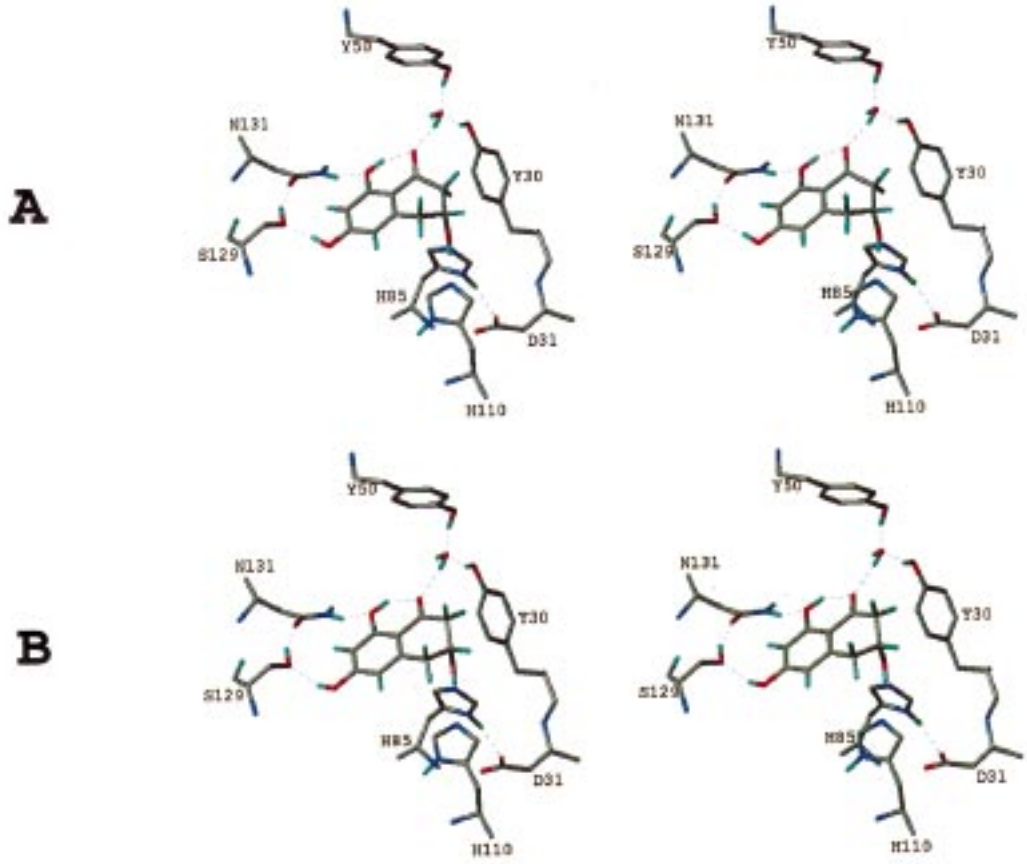

FIGURE 4: Models of scytalone in the SD active site: (A) syn-diaxial orientation; (B) anti-diaxial orientation.

EXPERIMENTAL PROCEDURES

Materials and General Methods. DDBO (*15*) and DHS (**3**; Figure 3) (*16*) were synthesized as described. Scytalone was purified from cultures of *rsy*$^-$ mutants of *M. grisea* (*3*). The enzymatic synthesis of vermelone from scytalone was accomplished essentially as described (*17*). UV/Vis spectrophotometric analyses were performed on HP 8452A or HP8453 diode array spectrophotometers (Hewlett-Packard). SDS−PAGE analyses of proteins were conducted by using a PhastSystem (Pharmacia, Uppsala, Sweden). Homogeneous wild-type SD (*18*) and 3HN reductase (*19*) were purified as described. Inhibition constants were determined as before (*8*). Crystallization at pH 7.5, data collection at 100 K, data processing, and refinement methods for the Y50F mutant complexed with inhibitor **2** were very similar to those reported (*8*). Molecular masses of SD and the mutants were determined using a Fisons VG Quattro II mass spectrometer with calibration against horse heart myoglobin as an external standard. Cysteine content of the enzymes was determined colormetrically using the thiol reagent, 5,5′-dithio-bis(2-nitrobenzoic acid), in the presence of 0.1% SDS at pH 8.0 with anhydrous cysteine-HCl as a standard. ^{1}H NMR and ^{13}C NMR were recorded on either a Varian VXR-300 NB or a Varian VXR-400-ND instrument. Preparations of **2** and **4** (Figure 3) can be found in Supporting Information.

Preparation of Scytalone Dehydratase Mutants. Cloning and generation of recombinant plasmids were carried out using standard methods (*20*). Mutant constructs were prepared by megaprimer mutagenisis (*21*) or more standard methods. For details of the constructs see Supporting Information. Following sequencing, the correct mutant SD expression plasmids were transformed into BL21(DE3) cells for protein expression. Cells containing expression vectors for Y30F, D31N, Y50F, Y30F/Y50F, H110N, N131A, or wild-type SD's were grown at 37 °C in LB medium in the presence of 100 mg/L ampicillin to between 0.5 and 0.7 OD_{600}. Induction was with 1 mM 1-(isopropylthio)-β-D-galactopyranoside, which was added 3 h before harvest. These SD's were produced predominately in the soluble fraction. H85N was produced predominately in inclusion bodies under these conditions. Successful production of H85N in the soluble fraction was accomplished by growing the cells at 30 °C for 3 h after induction. Purification of the mutant SD's was by hydrophobic interaction chromatography followed by anion-exchange chromatography essentially as described for wild-type SD (*18*).

The D31N mutation was introduced into an N-truncated form of SD, which lacks residues 3−9 (*22*). The N-truncation has no effect on SD catalytic properties. Attempts to produce D31N in the soluble fraction failed; hence this SD was refolded from the inclusion bodies. Lysed *Escherichia coli* cells containing D31N in 50 mM Tris-HCl, pH 7.5, 5 mM $MgCl_2$, 5 μg/mL RNAse, 5 μg/mL DNAse, and protease cocktail (COMPLETE; Boehringer Mannheim) were incubated 10−20 min at 22 °C until the extract was no longer viscous. Following centrifugation for 5 min at 18000*g*, the inclusion body-containing pellet was washed twice with extraction buffer by resuspending the pellet and recentrifuging. The final pellet was solubilized in 6 M guanidine-HCl, 0.1 M sodium phosphate, pH 7.0, and 20 mM DTT. The denatured protein (5 mL, 50 mg/mL) in guanidine-HCl buffer was refolded at 4 °C by adding it in 0.1 mL aliquots

to a stirred 1 L solution of 50 mM Tris-HCl, pH 7.5, and 1 mM DTT to achieve a final dilution of 200-fold. The diluted protein solution was concentrated in an Amicon ultrafiltration unit with a PM10 membrane before purifying the protein by anion-exchange chromatography (*18*).

Determination of Steady-State Kinetic Constants. Assay mixtures (0.5 or 1 mL) included 100 mM sodium phosphate, variable concentrations of scytalone (20−1000 μM), DDBO (10−4200 μM), or vermelone (30−400 μM) at pH 7.0 and 25 °C. Reactions (10−60 s) were initiated with enzyme and monitored continuously in 0.2 or 1 cm quartz cuvettes at the following substrate-dependent wavelengths: 352 nm ($\Delta\epsilon_{352} = 4100\ M^{-1}\ cm^{-1}$) for scytalone (*23*), 276 nm ($\Delta\epsilon_{276} = -5800\ M^{-1}\ cm^{-1}$) or 320 nm ($\Delta\epsilon_{320} = 1500\ M^{-1}\ cm^{-1}$) for DDBO (*15*), and 332 nm ($\Delta\epsilon_{332} = 5050\ M^{-1}\ cm^{-1}$) for vermelone (this work). Initial velocities were fit to eq 1 where

$$v = \frac{k_{cat}A}{K + A} \quad (1)$$

v is the observed initial velocity of the reactions, k_{cat} is maximum velocity, A is the substrate concentration, and K is the Michaelis constant.

Determination of Inhibitor to Active-Site Stoichiometries. Rates of catalysis were titrated with tight binding inhibitor **2** ($K_i = 9.0 \pm 0.7$ pM; Figure 3). Reactions (1 mL) included 100 mM sodium phosphate, pH 7.0, 0.5% DMSO, 0.3 mM DDBO, and at least 1 μM SD protomer. Inhibitor concentrations were varied in order to achieve 0−75% inhibition and the spectrophotometric data were fitted to eq 2, where v is

$$v = V\left(1 - \frac{I}{M}\right) \quad (2)$$

the observed rate of catalysis, V is the uninhibited rate of catalysis, I is the inhibitor concentration, and M is the total concentration of active sites. Stoichiometries of inhibitor binding per enzyme protomer were calculated by solving for the I intercept. Protomer concentrations were determined by using extinction coefficients at 280 nm for the proteins which were calculated by using the Peptidesort computer program within the Wisconsin Sequence Analysis Package (*24*). The calculated ϵ_{280} values were 48 850 $M^{-1}\ cm^{-1}$ for the wild-type, K73A, K73Q, D31N, H85N, H110A, H110N, S129A, and S129T SD's discussed in this work. A value of 47 570 $M^{-1}\ cm^{-1}$ was used for the Y30F and Y50F mutants and 46 290 $M^{-1}\ cm^{-1}$ for the Y30F/Y50F double mutant.

pH Studies. Steady-state kinetic parameters were measured at varying pH's. Values for k_{cat} and k_{cat}/K_m were fit to eq 3,

$$p = \frac{P}{1 + K_a/[H^+]} \quad (3)$$

which describes the titration of a single ionizable group when there is a decrease on the basic side. p represents the measured parameter, P is the pH-independent value for the parameter, $[H^+]$ is the proton concentration, and K_a is the acid dissociation constant for the group affecting catalysis. Buffers used when scytalone was the substrate were the following: pH's 6.26, 6.95, and 8.06 were 100 mM sodium phosphate; and pH's 8.90 and 9.50 were 90 mM sodium pyrophosphate and 10 mM sodium phosphate. Buffers used when DDBO was the substrate were as follows: pH's 6.10 and 7.01 were 100 mM sodium phosphate; pH's 6.95 and 7.0 were 90 mM sodium phosphate; pH 7.44 was 100 mM Hepes-NaOH; pH 6.98 was Mops-NaOH; pH 7.45 was 80 mM sodium phosphate and 20 mM sodium pyrophosphate; pH 7.95 was 90 mM Tris-HCl; pH 8.29 was 50 mM sodium phosphate and 50 mM sodium pyrophospate; pH 8.99 was 90 mM Ampso-NaOH; and pH's 9.49 and 9.99 were 90 mM Capso-NaOH.

*NMR Studies with Enzyme and ^{13}C-DHS **4**.* ^{13}C NMR spectra of 0.5 mM ^{13}C-DHS in 50 mM Tris HCl, pH 7.5, containing 20% D_2O and 5% ^{13}C-depleted D_6-DMSO in 1 mL were recorded in the absence and presence of 1 mM SD with a pulse width of 5.5 μs and a delay of 2.0 s between 4096 and 100 352 scans, respectively. A third ^{13}C NMR spectrum (4096 scans) was obtained after adding a 60 μL solution of 17.5 mM solution of **1** in ^{13}C-depleted D_6-DMSO to the SD-^{13}C-DHS solution: ^{13}C NMR (without SD), δ 39; (with SD), δ 41 (broad) and δ 39 (broad); (with SD and inhibitor **1**), δ 39.

Incubation of DHS (**3**) *with SD in D_2O*. Three buffers were prepared in D_2O: buffer A, 100 mM MES−NaOH, pD 6.0; buffer B, 100 mM sodium phosphate, pD 7.0; and buffer C, 100 mM sodium pyrophosphate, pD 9.0. Three 10 mg portions of DHS (*16*) were wetted with 0.02 mL of DMSO. Ten milliliters of buffer A was added to one, 10 mL of buffer B was added to a second, and 5 mL of buffer C was added to a third. The three samples were sonicated and filtered through a 0.2 micron filter, and each sample was split into two equal volumes. An aliquot (0.033 mL of 1.39 mM SD, 0.92 mg) in 50 mM Tris-HCl, pH 7.5, was added to one of each of the split samples to give an enzyme and a nonenzyme incubation of DHS at the 3 pD's. After incubation for 1 h at 25 °C, the samples were extracted twice with 2 volumes of ethyl acetate. The ethyl acetate layers were dried with Na_2SO_4 and evaporated under N_2. All of the samples exhibited the same NMR spectrum: ^{1}H NMR ($CDCl_3$) δ 2.05 (m, 2H), 2.85 (m, 2H), 2.85 (m, 2H), 6.2 (s, 2H), 12.8 (s, 1H).

Time Course Incubation of Scytalone with SD in D_2O. To a 1 mL solution of 5.0 mM scytalone in D_2O was added 10 μL of SD (4 μg) in 50 mM Tris-HCl, pH 7.0. Aliquots (10 μL) were removed at time points corresponding to before enzyme addition and 20, 60, 120, 180, and 360 s after the addition of enzyme. The aliquots were added to 1 mL solutions containing H_2O, acetonitrile, and formic acid (1:1:0.01 by volume) at 0−4 °C and subjected to electropspray ionization mass spectrometry. Positive scans were collected, and the ratios of the 195.25 and 196.25 amu peaks were compared at the individual time points to search for incorporation of deuterium into scytalone. The 360 s time point corresponded to approximately 50% conversion of scytalone to 3HN.

*Preparation of D_6-Scytalone **5***. Scytalone (0.1 mmol) was incubated in 20 mL of 100 mM sodium phosphate buffer in D_2O, pD 7.0, 1 mM $NADP^+$, and 10 mg of 3HN reductase under a nitrogen atmosphere at 25 °C. After 4 h, the equivalent of 5 mM NADPH, 10 mM glucose 6-phosphate, and 10 units of glucose 6-phosphate dehydrogenase was added to the reaction mixture without changing the D_2O composition. After an additional 1 h at 25 °C the reaction mixture was extracted thrice with equal volumes of ethyl acetate. The ethyl acetate layer was dried (Na_2SO_4), evaporated, and stored at −20 °C until use. EIMS of the material

indicated that the scytalone derivative had 6 deuterium atoms with no other significant species present. The pK_a values of D_6-scytalone and scytalone were determined spectrophotometrically by measuring 330 nm absorbencies versus pH. D_6-scytalone had a pK_a of 7.31 ± 0.004, similar to the value of 7.29 ± 0.015 determined for scytalone.

Measurements of Deuterium Kinetic Isotope Effects. Steady-state kinetic data for D_6-scytalone were measured side-by-side with scytalone as described above. Data were fit to eq 4 for the estimation of KIE's on k_{cat} and k_{cat}/K_m. ^DV

$$v = \frac{VA}{K(1 + f_i(^D(V/K) - 1)) + A(1 + f_i(^DV - 1))} \quad (4)$$

is the KIE on k_{cat}, $^D(V/K)$ is the KIE on k_{cat}/K_m, f_i is the fraction of isotope enrichment, and the other definitions are the same as in eq 1.

Single-Turnover Experiments. These were conducted using a stopped-flow instrument (Applied Photophysics; Leatherhead, U.K.) thermostated at 25 °C. The right syringe contained 1 mM SD in 100 mM sodium phosphate, pH 7.0, and the left syringe contained either 0.1 mM scytalone, 0.1 mM D_6-scytalone, 0.1 mM DDBO, or 0.1 mM vermelone. Equal volumes (0.06 mL) of the contents of each syringe were mixed to initiate reactions. Absorbencies of the reactions were monitored for 30 ms at 352, 320, or 332 nm for scytalone, DDBO, or vermelone reactions, respectively, and the data were fit to a single-exponential decay. Data were collected in triplicate or more for all four reactants.

Measurements of the Non-Enzyme-Catalyzed Rates of Dehydration for Scytalone, D_6-Scytalone, and DDBO. A 2 mL solution containing 100 mM sodium phosphate, pH 7.0, and 2.0 mM substrate was filtered through a 0.2 micron filter into a sterile tube. The solutions were incubated in a thermostated water bath at 25 °C. Aliquots (0.1 mL) were removed at time points for up to 60 days using a sterile pipettor and stored at −80 °C until use. The samples were analyzed in triplicate for remaining scytalone, D_6-scytalone, or DDBO by adding 30 μL of the sample to 970 μL of sodium phosphate, pH 7.0. For the scytalone- and D_6-scytalone-containing samples the absorbance at 352 nm was recorded before and after the addition of 4 μg of SD in 0.4 μL to the sample and the enzyme-catalyzed reaction had reached an end point (less than 1 min). For the DDBO-containing samples, the absorbance at 320 nm was recorded before and after the addition of 1 μg of SD in 0.1 μL to the sample and the enzyme-catalyzed reaction had reached an end point (less than 1 min). The delta absorbance data were fit to an equation describing a first-order decay with a zero endpoint.

Equilibrium of Scytalone-3HN within the Active Site. Reactions (0.5 mL) contained 1.4 mM SD, 0.19 mM scytalone, 100 mM sodium phosphate, pH 7.0, at 25 °C. After 70 s, the reactions were quenched with 10 μL of 1 M H_2SO_4, bringing the pH to 2.5. The mixture was extracted four times with 2 mL volumes of ethyl acetate, and the ethyl acetate layers were dried under a N_2 stream. The residue was dissolved in 1 mL of 100 mM sodium phosphate, pH 7.0, and was analyzed enzymatically for scytalone as described above. The extract was found to have a UV/vis spectrum corresponding to 3HN, and no scytalone could be detected.

Burst Experiments. Pre-steady-state followed by steady-state experiments were conducted using an Applied Photophysics stopped-flow instrument thermostated at 6.8 °C. The left syringe contained 2 mM scytalone in 100 mM sodium phosphate, pH 7.0. The right syringe contained 0.050 mM SD in 100 mM sodium phosphate, pH 7.0. Absorbencies of the reactions were monitored at 352 nm for 100 ms, and the data were fit to a single exponential followed by a steady state. Data were collected in triplicate.

Table 1: Molecular Masses, Cysteine Content, and Active-Site Titrations with Inhibitor 2 of Wild-Type and Mutant Scytalone Dehydratases

enzyme	molecular mass (Da): electrospray ms value	molecular mass (Da): predicted value[a]	cysteine content (mol of cysteine/mol of enzyme)[b]	molar ratio (inhibitor **2**/enzyme)[b,c]
wild-type	20118.2	20118.6	1.05 ± 0.05	0.99 ± 0.03
K73A	20060.9	20061.5	1.08 ± 0.02	1.1 ± 0.02
K73Q	20118.1	20117.5	1.07 ± 0.01	1.0 ± 0.04
D31N[d]	19346.7	19344.8	1.14[e]	0.87 ± 0.05[f]
D31N	19481.5	19476.0[f]		
D31N	19402.7	19504.0[g]		
H85N	20096.1	20095.5	1.04[e]	0.64 ± 0.04
H110A	20051.0	20052.5	1.02 ± 0.05	0.92 ± 0.02
H110N	20096.6	20095.5	1.02 ± 0.04	1.3 ± 0.08
N131A	20075.8	20075.5	0.98 ± 0.03	1.1 ± 0.03
Y30F	20102.0	20102.5	1.00 ± 0.05	1.1 ± 0.03
Y50F	20102.2	20102.5	0.90 ± 0.01	1.0 ± 0.07
Y30F/Y50F	20086.0	20086.6	1.12[e]	1.1 ± 0.01
S129A	20102.0	20102.6	0.93 ± 0.09	1.0± 0.02
S129T	20131.9	20132.6	1.16[e]	0.81 ± 0.02

[a] Predicted mass for the protomer minus the N-terminal methionine. [b] Enzyme protomer. [c] Standard errors from the fits to eq 2 are indicated. [d] An N-truncated SD (lacking residues 3−9) was used to prepare the D31N mutant. [e] Single determination. [f] Predicted mass for the protomer including the N-terminal methionine. [g] Predicted mass for the protomer including the N-terminal *N*-formylmethionine.

RESULTS

Site-Directed Mutagenesis and Analysis of Mutant Constructs. All mutant cDNA's were completely sequenced to confirm the fidelity of the PCR reaction. Expressed mutant proteins were purified to homogeneity as judged by SDS−PAGE. EIMS indicated that the mutants had the correct molecular weights (Table 1). The cysteine content (one per protomer) was taken as another indication of protein purity. Active-site titration with the inhibitor **2** (K_i = 9.0 ± 0.7 pM) was used as an indicator of the fraction of properly folded recombinant protein (Table 1). Only the H85N mutant diverged substantially below one active site per protein monomer, and corrections to catalytic constants were made on the basis of these titrations.

Steady-State Kinetic Parameters. k_{cat} for the wild-type SD is limited by events after the dehydration reaction by a factor of 6 when scytalone is the substrate and very little when DDBO is the substrate (see below). k_{cat} values of mutant enzymes severely compromised in catalysis should reflect the true rates of dehydration. Steady-state kinetic constants for SD-catalyzed dehydrations of scytalone and the synthetic substrate DDBO are presented in Tables 2 and 3, respectively. There was one residue (K73) that, when mutated to alanine and glutamine, has no effect on k_{cat} or K_m for either substrate.

Replacement of either H85 or H110 with an asparagine residue greatly decreases catalytic efficiency. It was impossible to measure the turnover of scytalone with the H85N

Table 2: Steady-State Kinetic Parameters for Scytalone Dehydratase and Mutants with Substrate Scytalone at pH 7.0 and 25 °C[a]

enzyme	k_{cat}(scytalone) (s^-)	k_{cat}/K_m(scytalone) ($\mu M^{-1}s^{-1}$)	K_m(scytalone) (μM)
wild-type[b]	73 ± 8	2.2 ± 0.3	33 ± 3
K73A	80 ± 2	2.0 ± 0.1	40 ± 2
K73Q	76 ± 2	2.0 ± 0.1	38 ± 4
D31N[c]	0.014 ± 0.002	$1.0 \times 10^{-4} \pm 3 \times 10^{-5}$	140 ± 60
H110A	$0.011 \pm 4 \times 10^{-4}$	$4.7 \times 10^{-4} \pm 6 \times 10^{-5}$	24 ± 4
H110N	0.039 ± 0.001	$5.7 \times 10^{-4} \pm 2 \times 10^{-5}$	68 ± 5
N131A	0.82 ± 0.02	$3.5 \times 10^{-3} \pm 2 \times 10^{-4}$	240 ± 20
Y30F	8.0 ± 0.2	0.14 ± 0.006	58 ± 4
Y50F	0.15 ± 0.004	$2.9 \times 10^{-3} \pm 2 \times 10^{-4}$	50 ± 4
Y30F/Y50F	$7.0 \times 10^{-3} \pm 4 \times 10^{-4}$	$3.0 \times 10^{-4} \pm 5 \times 10^{-5}$	23 ± 5
S129A	0.94 ±0.03	$4.3 \times 10^{-3} \pm 2 \times 10^{-4}$	220 ± 20
S129T[d]	0.61 ± 0.08	$8.0 \times 10^{-4} \pm 7 \times 10^{-5}$	770 ± 160

[a] Standard errors from the fits to eq 1 are indicated with the values. [b] Means and standard deviations from 7 determinations. [c] Based on active-site titration.

Table 3: Steady-State Kinetic Parameters for Scytalone Dehydratase and Mutants with Substrate DDBO at pH 7.0 and 25 °C[a]

enzyme	k_{cat}(DDBO) (s^{-1})	k_{cat}/K_m(DDBO) ($\mu M^{-1}s^{-1}$)	K_m(DDBO) (μM)
wild-type[b]	400 ± 9	27 ± 2	15 ± 1
K73A	380 ± 6	18 ± 1	21 ± 1
K73Q	340 ± 8	21 ± 1	16 ± 1
D31N[c]	4.6 ±0.2	$2.4 \times 10^{-3} \pm 1.0 \times 10^{-4}$	1,900 ±170
H85N[c]	$8.2 \times 10^{-3} \pm 8 \times 10^{-4}$	$1.4 \times 10^{-3} \pm 8 \times 10^{-4}$	5.7 ± 4
H110A	0.24 ± 0.01	0.064 ± 0.02	3.8 ± 1
H110N	1.8 ± 0.05	0.16 ± 0.02	12 ± 2
N131A	120 ± 7	0.20 ± 0.01	600 ± 70
Y30F	28 ± 0.6	1.9 ± 0.1	15 ± 1
Y50F	1.9 ± 0.03	0.17 ± 0.01	11 ± 1
Y30F, Y50F	0.050 ± 0.003	0.011 ± 0.003	4.6 ± 1
S129A	390 ± 11	17 ± 1.0	22 ± 2
S129T[d]	580 ± 30	3.3 ± 0.2	170 ± 20

[a] Standard errors from the fits to eq 1 are indicated with the values. [b] Means and standard deviations for 8 determinations. [c] Values corrected for active-site content.

mutant in the continuous spectrophotometric method employed for the other mutant enzymes; on the basis of the assay sensitivity it is estimated that k_{cat} is reduced at least 100000-fold. A low level of enzyme activity was detected using the alternate substrate, DDBO, sufficient for measuring kinetic parameters. The k_{cat} for this substrate was lowered by 50000-fold in comparison to wild-type SD, while K_m was reduced 3-fold. Smaller effects are seen upon mutation of H110. Replacing histidine with alanine at this position results in 1900- and 200-fold reductions in turnover rates with scytalone and DDBO as substrates, respectively. The H110N mutant had k_{cat} values reduced by 6600- and 1800-fold for the same substrates. Substrate binding is not greatly affected by either H110 mutation. The effect of replacing Y30 and Y50 with phenylalanine is also on catalysis rather than substrate binding, with the Y50 mutation having a larger effect. The Y30F mutant had k_{cat} values 9- and 14-fold lower for scytalone and DDBO, respectively, while the Y50F mutant showed turnover rates reduced by 500- and 200-fold, respectively. The combined effect of the two mutations is roughly additive for the two individual mutations, the double mutant having 0.01% of the wild-type activity with both substrates without appreciably affecting substrate binding.

Mutation of three residues produced effects on both substrate binding and catalysis. Replacement of N131 with alanine decreased turnover by nearly 90-fold and increased K_m 8-fold with scytalone as the substrate. With DDBO, the effect on catalysis is less but the loss of binding affinity is greater. Similar but larger effects are seen upon mutation of D31 to an asparagine: with scytalone, catalysis is reduced 5000-fold and substrate affinity about 4-fold. With DDBO, turnover and substrate affinity are both reduced approximately 100-fold. S129 was changed to alanine and threonine residues. Replacement with alanine resulted in a 80-fold loss in k_{cat} and a 7-fold increase in K_m with scytalone. With DDBO there was no loss in k_{cat} and a 1.5-fold increase in K_m. Replacement of S129 with threonine resulted in a 120-fold decrease in k_{cat} and a 23-fold increase in K_m with scytalone. With DDBO, k_{cat} and K_m were elevated by a factors of 1.5 and 11, respectively.

Table 4: Steady-State Kinetic Parameters for Scytalone Dehydratase and Mutants with Substrate Vermelone at pH 7.0 and 25 °C[a]

enzyme	k_{cat}(vermelone) (s^{-1})	k_{cat}/K_m(vermelone) ($\mu M^{-1}s^{-1}$)	K_m(vermelone) (μM)
wild-type	73 ± 3	2.4 ± 0.3	31 ± 4
H110N	0.29 ± 0.01	$1.7 \times 10^{-3} \pm 0.5 \times 10^{-5}$	180 ± 9
N131A	50 ± 6	$3.6 \times 10^{-2} \pm 2.0 \times 10^{-3}$	1400 ± 200
Y50F	2.8 ± 0.08	$3.5 \times 10^{-2} \pm 2.0 \times 10^{-3}$	78 ± 5
S129A	180 ± 6	3.5 ± 0.3	51 ± 5

[a] Standard errors from the fits to eq 1 are indicated with the values.

Studies on substrate vermelone were limited due to its availability. Kinetic parameters obtained for the wild-type SD and mutant enzymes are listed in Table 4. The wild-type SD has steady-state kinetic parameters with this substrate that are very similar to those with scytalone. Replacement of H110 with asparagine caused a 250-fold drop in k_{cat} and a 6-fold increase in K_m. The N131A mutation caused a 40% loss in k_{cat} and a 45-fold increase in K_m. The Y50F change decreased k_{cat} 26-fold and increased K_m 2.5-

Table 5: Relative Substrate Specificities of Scytalone Dehydratase and Mutants for Scytalone, Vermelone, and DDBO at pH 7.0 and 25 °C[a]

enzyme	k_{cat}/K_m(vermelone)/ k_{cat}/K_m(scytalone)	k_{cat}/K_m(DDBO)/ k_{cat}/K_m(scytalone)	k_{cat}/K_m(DDBO)/ k_{cat}/K_m(vermelone)
wild-type	1.1	12	11
H110N	3.0	290	97
N131A	10	570	57
Y50F	12	59	4.8
S129A	820	4000	5.0
S129T	nd[b]	4100	nd
Y30F	nd	14	nd
Y30F, Y50F	nd	37	nd
D31N	nd	24	nd
H110A	nd	140	nd
K73A	nd	9.0	nd
K73Q	nd	11	nd

[a] Ratios of the values found in Tables 2, 3, and 4. [b] Not determined.

fold. The S129A mutation increased k_{cat} 2.5-fold and increased K_m 1.6-fold.

The mutations alter relative substrate specificities for scytalone, vermelone, and DDBO as indicated in Table 5. With the exception of the K73 mutants, the mutant enzymes lost specificity for scytalone more than for the other two substrates in comparison to wild-type SD. The largest changes in relative specificities (comparing DDBO and vermelone to scytalone) were with the S129 mutants. This result helps orient scytalone in the active site of SD with the C6 hydroxyl directed toward S129. Relative specificities (comparing DDBO and scytalone) were also increased significantly in the H110 and N131 mutants. Among the mutants examined, only H110N and N131A preferred DDBO significantly over vermelone in comparison to wild-type SD.

X-ray Structure of the Y50F Mutant. The Y50F mutant was cocrystallized with potent inhibitor **2** ($K_i = 9.0 \pm 0.7$ pM) using conditions that were developed for crystallizing an N-truncated SD (*8*). The crystal diffracted well, and a data set was collected to 1.9 Å. After molecular replacement, the data was put through only one cycle of refinement where Y50 was replaced with an alanine in the model. It is clear from the electron density of this initial map that Y50 had been changed to a phenylalanine (Figure 5). It is also clear that both of the active-site water molecules are retained, including the one that is hydrogen bonded to Y30 and the inhibitor carbonyl. In many structures of wild-type SD, this water molecule is hydrogen bonded to Y30 as well as Y50 and the inhibitor. The presence of this water molecule is likely responsible for the residual catalytic activity in the Y50F mutant.

pH Studies. We are able to study the effect of pH on catalysis above pH 6, but as the medium becomes more acidic, SD becomes irreversibly inactivated: when the enzyme is incubated at pH 6.0 for 10 s followed by raising the pH to 7.0 (where the enzyme is fully stable), there is little catalytic activity remaining. It was found that the pH inactivation was protected by substrates scytalone and DDBO (data not shown), so it seems likely that the low-pH conditions disturb the active site (possibly H85 and H110, which are neighbors). For the dehydration of scytalone, pH 7 is optimal (Figure 6). As the pH increases, k_{cat}/K_m drops with a pK_a of 7.9 due to deprotonation of the substrate; the C6 hydroxyl of scytalone has a p$K_a = 7.29 \pm 0.01$. The observed pK_a of 7.9 is likely elevated over its true value of 7.3, in part because of enzyme inactivation at lower pH's that prevents a true (and higher) value for the pH-independent value for k_{cat}/K_m to be realized. Substrate stickiness is an unlikely factor, as a large KIE on k_{cat}/K_m was measured (see below). k_{cat} is constant over the pH range, indicating that the drop in k_{cat}/K_m is due to the poor binding of the anionic form of scytalone. In contrast, there is no drop in k_{cat}/K_m for DDBO until pH 9 is reached (Figure 7). DDBO has a pK_a $\geq$ 11 (*15*), and therefore the drop in k_{cat}/K_m having a pK_a of 9.3 can be attributed to the protein. k_{cat} is constant over the pH range, so the pK_a of 9.3 for k_{cat}/K_m may be attributed to an enzyme residue that needs to be protonated in order for substrate to bind.

Enolization Studies. ^{13}C-labelel DHS was incubated with SD to provide evidence for enolization, which would represent a partial reaction in the dehydration of scytalone in an E1cb-like mechanism. At the concentrations used and with a $K_i = 10$ μM, most of the ^{13}C-DHS should have been complexed with the enzyme. There was a dramatic broadening of the resonance on mixing with SD supporting this, and a three-day accumulation of data was required in order to visualize the ^{13}C resonance. The slight downfield shift for the ^{13}C resonance of DHS when bound to SD ($\delta = 41$ ppm) is consistent with the keto form of the molecule. A second peak at $\delta = 39$ ppm suggests a second binding mode for the keto form or a trace of unbound ^{13}C-DHS. There was no evidence of an enol form of the inhibitor, as might have been seen with a resonance between δ 100 and 130 ppm. However, it is estimated that a minimum of 15% of the ^{13}C-DHS would need to be present in the enol form in order to be detected. Adding inhibitor **1** displaced ^{13}C-DHS from the SD binding pocket as observed in the regeneration of a sharp resonance at δ 39. Incubations (1 h) of DHS with SD in buffered D_2O at pD's 6, 7, and 9 followed by its reisolation showed no deuterium incorporation α to the carbonyl by NMR analysis.

It is possible that, although SD does not accept DHS as a substrate for enolization, it does induce an enolization of scytalone that could be detected. Running the enzyme-catalyzed dehydration in D_2O to 50% completion and reisolation of scytalone showed no deuterium incorporation from EIMS analysis. The ratios (195.25/196.25) of scytalone parent ions were 4.40, 4.38, 4.45, 4.38, 4.44, and 4.44 at times 0, 20, 60, 120, 180s and 360 s after adding enzyme to the reaction, whereas the ratio (177.14/178.24) of 3HN parent ions changed from 2.34 at 20 s to 0.59 at 360 s, showing that the reaction was proceeding and that the product was incorporating deuterium as expected. These results do not preclude the possibility that the enzyme removes a proton α to the carbonyl and returns the proton without exchange with solvent.

D_6-Scytalone and Pre-Steady-State Studies A KIE of 2.7 was measured for k_{cat}, and a KIE of 4.2 was measured for k_{cat}/K_m (Table 6). The larger KIE for k_{cat}/K_m over that of k_{cat} suggests that an event after the first irreversible step (dehydration) is rate-limiting to k_{cat}. Pre-steady-state experiments measured a rate of 430 s^{-1} as the single-turnover rate with scytalone (k_2 of Scheme 2), a value that is 6-fold higher than that of the steady-state k_{cat} and about equal to the k_{cat} for DDBO. Single-turnover experiments with DDBO and vermelone gave rates of 410 ± 30 and 430 ± 60 s^{-1} for the respective substrates indicating, that the three substrates for

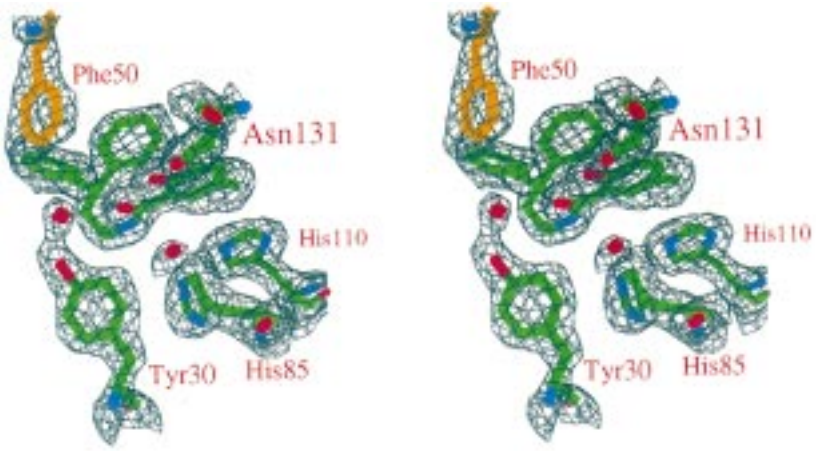

FIGURE 5: Stereoview of the electron density map around the active site of the Y50F mutant of scytalone dehydratase: $2|F_o| - |F_c|$.

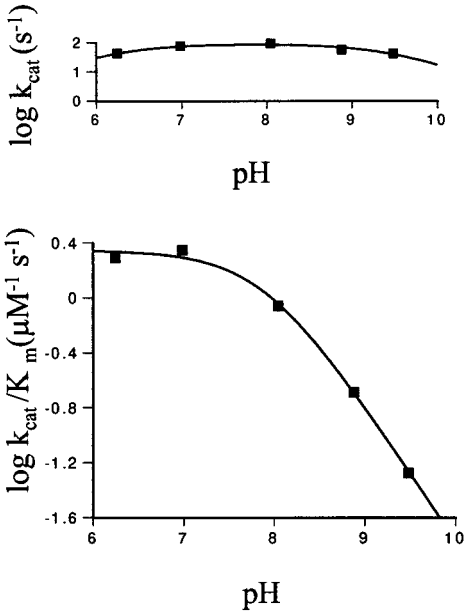

FIGURE 6: pH dependence of steady-state kinetic parameters of scytalone dehydratase with substrate scytalone: top panel, k_{cat} versus pH; lower panel, k_{cat}/K_m versus pH. A pK_a of 7.90 ± 0.05 was determined from the fit to eq 3.

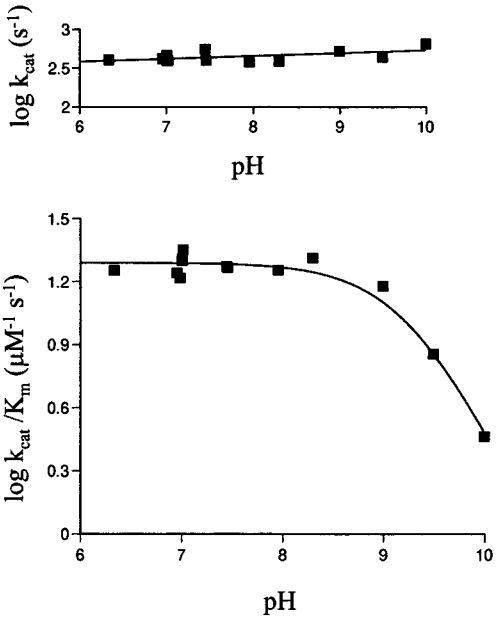

FIGURE 7: pH dependence of steady-state kinetic parameters of scytalone dehydratase with DDBO: top panel, k_{cat} versus pH; lower panel, k_{cat}/K_m versus pH. A pK_a of 9.27 ± 0.05 was determined from the fit to eq 3.

SD have nearly equal values for k_2. The KIE measured in the pre-steady state was 3.6 with D_6-scytalone (Table 6), a KIE that is similar to that of k_{cat}/K_m. The effect of D_6-scytalone on the kinetic parameters of two site-directed mutants was measured. KIE's on k_{cat} and k_{cat}/K_m were 4.8 ± 0.4 and 5.8 ± 0.8, respectively, for the Y50F mutant and 4.6 ± 0.4 and 4.3 ± 0.9, respectively, for the N131A mutant.

For the SD-mediated dehydration of scytalone, a burst in pre-steady state to steady state is difficult to measure at 25 °C because the substrate absorbency properties limit the usable concentrations and because k_2 is quite large. Therefore, we conducted the burst experiments at 6.8 °C with scytalone 40-fold more concentrated than enzyme. The observed burst had an amplitude equal to 22 ± 3 μM, similar to the enzyme concentration (25 μM). Since the single-turnover rate is a function of k_2 and k_{-2}, we measured the substrate−product equilibrium constant at 25 °C as a means of arriving at a value for k_{-2}. The incubation included 1.4 mM SD and 0.19 mM scytalone, ensuring that substrate scytalone and product 3HN would be fully bound. After extraction, all of the material was found to be 3HN. Given a lower limit of measurement of 1 nmol scytalone by our methods, the value for k_{-2} is estimated as at least 190-fold smaller than k_2.

Non-Enzyme-Catalyzed Rates for Reactions with Scytalone, D_6-Scytalone, and DDBO. Scytalone and DDBO were incubated at pH 7.0 and 25 °C in 0.1 M sodium phosphate buffer, and the rates of dehydration were measured in the absence of enzyme. Scytalone was considerably more stable than DDBO. The rate for scytalone dehydration was 1.17 ± 0.07 × 10^{-7} s^{-1}, while that for DDBO was 5.23 ± 0.09 × 10^{-6} s^{-1}. The KIE observed with D_6-scytalone was 1.24 ± 0.08. Incubations of scytalone in 0.1 M sodium phosphate at pD 7.0 in D_2O indicated that a C2 hydrogen exchanged with solvent with a half-life of about 1 day, about 70-fold more rapid than the dehydration rate.

DISCUSSION

Reactions Off the Enzyme. The non-enzyme-catalyzed dehydration rates for scytalone and DDBO were well-differentiated. k_{non}(scytalone) was 45-fold slower than k_{non}-(DDBO), and it is likely that the anomeric effect afforded

Table 6: Steady-State and Pre-Steady-State Kinetic Parameters for Scytalone Dehydratase Acting on Scytalone and D6-Scytalone at pH 7.0 and 25 °C[a]

kinetic parameter	value	kinetic parameter	value
k_{cat}(scytalone) (s^{-1})	69 ± 3	k_{cat}(D_6-scytalone) (s^{-1})	26 ± 1
k_{cat}/K_m(scytalone) (μM^{-1} s^{-1})	2.7 ± 0.3	k_{cat}/K_m(D_6-scytalone) (μM^{-1} s^{-1})	0.65 ± 0.05
K_m(scytalone) (μM)	26 ± 3	K_m(D_6-scytalone) (μM)	40 ± 4
k_{cat}(scytalone)/k_{cat}(D_6-scytalone)	2.7 ± 0.3	k_{cat}/K_m(scytalone)/k_{cat}/K_m(D_6-scytalone)	4.2 ± 0.9
k_2(scytalone)[b] (s^{-1})	430 ± 20	k_2(D_6-scytalone)[b] (s^{-1})	120 ± 3
k_2(scytalone)/k_2(D_6-scytalone)[b]	3.6 ± 0.2		

[a] Unless indicated, values are from steady-state measurements. Standard errors from the fits to eq 1 are indicated. [b] Values from single-turnover measurements.

Scheme 2. The Catalytic Cycle of Scytalone Dehydratase

$$E \underset{k_{-1}}{\overset{k_1[S]}{\rightleftharpoons}} ES \underset{k_{-2}}{\overset{k_2}{\rightleftharpoons}} EP \underset{k_{-3}[P]}{\overset{k_3}{\rightleftharpoons}} E$$

by DDBO is largely responsible for a more rapid rate of dehydration. The non-enzyme-catalyzed dehydration rate for D_6-scytalone had a KIE of 1.2. The C2 hydrogens of scytalone exchanged more rapidly with solvent in comparison to the rate of dehydration. Thus, the solvolytic dehydration of scytalone is through an E1cb path as represented in Scheme 1. The measured KIE is likely a combination of primary and secondary effects, the primary effect being severely dampened. The mechanism for the solvolytic dehydration of DDBO is less well-established with respect to the experimental information. Examination of the exchange of its Cα hydrogens with solvent is noninformative because the reversible opening and closing of the pyranone ring of DDBO is fast; the opening unveils a highly enolizable β-keto aldehyde that exchanges the α-hydrogens rapidly with D_2O. However, the anomeric carbon atom of DDBO would be expected to enhance the rate of dehydration most in an E1cb mechanism. If one assumes that the ring-closed form of DDBO enolizes at the same rate as scytalone, then the rates for enolization and dehydration of DDBO become similar to one another.

The Anomeric Effect of DDBO. Previously, it was reasoned that, since the k_{cat} for DDBO is 6-fold larger than that for scytalone, there is an anomeric effect on the wild-type enzyme-catalyzed dehydration of DDBO (*15*). In this work we determined from single-turnover experiments that k_2 values (Scheme 2) for scytalone, vermelone, and DDBO are about the same (400 s^{-1}) and that the k_{cat}(scytalone) of 73 s^{-1} is likely limited by a subsequent event (k_3). Since k_{cat} for DDBO is equal to k_2 for DDBO, k_3 for this substrate must be considerably larger than 400 s^{-1}. One difference between the products of dehydrations of DDBO and scytalone is the C3 hydroxyl of the latter's dehydration product (3HN), which can form a hydrogen bond to S129 and perhaps account for a slower off-rate-limiting k_3. Refuting this notion is that the measured k_{cat} and k_2 values for vermelone, whose product also lacks the C3 hydroxyl, are about the same as those for scytalone. A second difference is that after dehydration, scytalone and vermelone must undergo a tautomerization reaction from a tetralenone structure to the naphthol (see below and Scheme 1) whereas DDBO does not.

It is calculated that k_{cat}(scytalone)/k_{non}(scytalone) is 6×10^8, whereas k_{cat}(DDBO)/k_{non}(DDBO) is 8×10^7. Catalytic proficiencies [(k_{cat}/K_m)/k_{non}] are 2.3×10^{13} and 5.1×10^{12} M^{-1} for scytalone and DDBO, respectively, illustrating that the enzyme lowers the activation energy barrier more efficiently for its natural substrate than for the synthetic one. That the lowering of the activation energy barrier by SD for DDBO is less than that for scytalone indicates that the anomeric carbon atom is important to the dehydration mechanism off the enzyme but not on the enzyme. The leveling of the activation energy required for the dehydration of scytalone as mediated by SD is smaller than that provided by fumarase which catalyzes an analogous elimination reaction (*25*), but SD is nonetheless quite impressive as a catalyst. In addition to providing catalytic residues to promote the dehydration of scytalone, the SD active site is arranged to lower the activation barrier by recognition of either the anti-diaxial or syn-diaxial conformers of scytalone (Figure 4), the latter conformer having more appeal because it orients the axial C2 hydrogen more satisfyingly toward the basic H85.

Kinetic Isotope Effects. KIE's on k_{cat} and k_{cat}/K_m offered the first suggestion that a step following catalytic dehydration by SD may be rate-limiting to k_{cat}(scytalone). We measured single-turnover rates to find the magnitude of k_2 relative to k_{cat}. The first-order decay measurements for determining k_2 are influenced by the value for k_{-2}, but since the product−substrate equilibrium constants in the enzyme active site and in solution lie far in the direction of product 3HN (at least 190-fold), the value from the single turnover should closely approximate k_2. However, when one calculates the steady-state value for k_{cat}(scytalone)/k_{cat}(D_6-scytalone) using eq 5

$$k_{cat}(H)/k_{cat}(D) = (k_2(H)/k_2(D)(k_2(D) + k_3)/(k_2(H) + k_3) \quad (5)$$

with the pre-steady-state values for k_2(scytalone) and k_2(D_6-scytalone) in Table 6 and assuming a rate of 100 s^{-1} ($> k_{cat}$ for scytalone) for k_3, there is a discrepancy. The measured value for k_{cat}(scytalone)/k_{cat}(D_6-scytalone) is 2.7, and the value calculated from eq 5 is 1.5. It appears that k_3 is an isotope-sensitive step invalidating the use of eq 5. We speculate here that dehydration affords an enone that tautomerizes relatively slowly and that the dehydrated product (the enone) of D_6-scytalone would present a primary deuterium KIE on the tautomerization. The half-life for D_2O exchange is 7 min for 4HN which exists as a 7:3 mixture of the phenolic to keto forms in acetone (*26*). Since hydrogen bonding stabilizes the keto forms of *m*-diphenols (*27*), it is reasonable that tautomerization of the enone form of 3HN is somewhat slow. Supporting this is that DDBO, which does not tautomerize after dehydration, has a $k_{cat} = 400$ s^{-1}, similar to the value of k_2 on the enzyme. The timing and nature of

the events (tautomerization and product release) after k_2 await more detailed experimentation with substrate scytalone. The pre-steady-state value for k_2(scytalone)/k_2(D_6-scytalone) is 3.6, which is too large for a secondary KIE in mechanisms that do not have C2 deprotonation in the transition state. That a full primary KIE on k_2 of 6 or greater is not observed is understandable within any mechanism involving rate-limiting deprotonation, as the observed KIE would be dampened by other catalytic events, mainly the elimination of hydroxide.

Site-Directed Mutants. The kinetic parameters for the mutant enzymes indicate that all of the side chains examined here have critical roles in catalysis with the exception of K73. The certainty that K73 has no role in catalysis is consistent with the observations from numerous crystal structures indicating that the residue does not change its position (from its orientation toward bulk solvent away from the active site) enough to relocate it even close to the active site (*5*, *8*, *22*). The K73 mutant data also places certain doubts on the proposed anti elimination mechanism, as there remains no other enzymic residues near C2 of scytalone to serve as a general base. For such an elimination to occur on the enzyme, the C2 hydrogen must be accepted by bulk water which would require organization of the solvent to greatly increase its basicity.

Substrate specificity studies on the two S129 mutants help assign the orientations of scytalone within the active site as shown in Figure 4. S129A was designed to remove a hydrogen bond with the C6 hydroxyl of scytalone. Conversely, since vermelone and DDBO lack the analogous hydroxyl, the effect of the mutation on the two substrates was expected to be minimal. This was borne out as k_{cat}/K_m was severely compromised for scytalone but not for substrates DDBO and vermelone in comparison to wild-type SD. About a 10-fold increase in the K_m(scytalone) may be attributed to the loss of a hydrogen bond from S129. That k_{cat}(scytalone) is severely compromised in S129A suggests that the mutation perturbs productive binding of this substrate, perhaps by forming a hydrogen bond between the side chain of N131 and the C6 hydroxyl of scytalone. This makes scytalone an inappropriate substrate for interpreting k_{cat} with respect to S129A. It is a curiosity that the recently reported sequence of SD from *Aspergillus fumigatus* (*28*) places an alanine in the position corresponding to the S129 of *M. grisea* SD. This change perhaps makes the *A. fumigatus* SD a vermelone-specific dehydratase, thus raising questions on the melanin biosynthetic pathway in this organism. There is only one known dehydratase in *M. grisea*, and it processes both scytalone and vermelone efficiently. S129T maintains the capability for hydrogen bonding with the C6 hydroxyl of scytalone but places a steric impediment into the portion of the binding pocket where the hydroxyl is situated. Accordingly, the K_m for scytalone is increased 20-fold by the S129T mutation. Similar to S129A, k_{cat} is severely compromised with scytalone but not with DDBO. Unlike the S129A mutant, S129T has a 10-fold increased K_m for DDBO, which is attributed to the increased steric hindrance.

It was proposed that Y30 and Y50 assist the protonation of the substrates' carbonyl through the water molecule (*5*, *14*). It was not predictable that Y50F mutant would be more debilitated in k_{cat} than the Y30F mutant, and it required experimental data to reveal this difference. The KIE for k_{cat}/K_m with D_6-scytalone was larger for Y50F (5.8) than that for wild-type SD (4.2), consistent with the role of Y50 in lowering the energy barrier for the deprotonation of C2. That the two tyrosine mutants lower k_{cat} supports the hypothesis that they serve in concert with the water molecule to protonate the substrates' carbonyl groups. This protonation serves to substantially lower the pK_a of the methylene α to the carbonyls of substrates. The unique aspect of having a water molecule relay the effects of two tyrosines for the proton donation represents an opportunistic adaptation by the enzyme. Only one lone pair of electrons is available on the carbonyl oxygen for coordination by the water molecule, yet both tyrosines serve as proton donors as revealed in the additive nature of the k_{cat} effects of the single mutations in the Y30F/Y50F double mutant.

We speculated that N131 positions substrates for productive binding and helps protonate their carbonyl through donation of a hydrogen to the phenolic oxygen atom. The finding that k_{cat} is decreased and that K_m is raised by the N131A mutation with the three substrates is consistent with this dual role. However, the more severe loss in k_{cat}(scytalone) in comparison to the modest losses in k_{cat}(DDBO) and k_{cat}(vermelone) suggests that the primary role of N131 is in substrate orientation and that N131A causes nonproductive binding with substrate scytalone, resulting in the large losses in k_{cat}. The KIE for k_{cat}/K_m with D_6-scytalone was about the same for N131A (4.3) as that for wild-type SD (4.2), consistent with N131 having little impact on the deprotonation of C2. H110 is thought to have a role in stretching the C3 carbon−oxygen bond by sharing a hydrogen bond with the hydroxyl leaving group. Consistent with this role, the H110A and H110N mutants have large decreases in k_{cat} and only minor changes in K_m with the substrates. H85 and D31 form a dyad to increase the basicity of the H85 imidazole. Consistent with the dual role of H85 as a general base and a general acid in the syn elimination mechanism, the H85N mutant was compromised by >100000- and 50000-fold in k_{cat} for substrates scytalone and DDBO, respectively, while having minor effects on K_m for DDBO (K_m was not measured for scytalone). The D31N mutant has devastating effects on both k_{cat} and K_m for both substrates scytalone and DDBO, likely resulting from losses of the native side chain roles in increasing the basicity of H85 and in organizing the active site through its participation in an extensive hydrogen-bonding network. D31 cannot form a direct interaction with the substrate, and its role in catalysis is mediated through the enhanced basicity of H85. His-Asp dyads are well-recognized for their roles in serine proteases where they serve to deprotonate a serine hydroxyl for the addition to a peptide bond and in other enzymes [e.g., aconitase (*29*) where it protonates a leaving hydroxyl group].

The Anomeric Effect of DDBO Revisited. Large differences in substrate specificities against the wild-type and mutant enzymes were observed. Specificity for substrate scytalone was eroded more in the mutants than for the other two substrates. This is reconciled for the S129 and N131 mutants by the C6 hydroxyl of scytalone causing nonproductive binding as discussed above. Therefore, if one wanted to examine the anomeric effect of DDBO on catalysis, it would be a mistake to compare substrates DDBO and scytalone. It would be more appropriate to compare DDBO and vermelone, substrates which differ by a methylene for an oxygen atom, against mutations in SD that affect turnover rather than

substrate binding. This leaves two mutant enzymes (H110N and Y50F) for comparison with wild-type SD. H110 and Y50 may be considered as having opposite-spectrum roles in the enzyme-catalyzed dehydrations with regard to stretching the C3 carbon−oxygen bond (providing E1 character) and assisting enolization (providing E1cb-like character), respectively, corresponding to two theoretical partial reactions on the enzyme. The expectation is that the mutations which damage the ability to stabilize the developing negative charge on the leaving hydroxyl group would prefer DDBO and its anomeric carbon over vermelone, while those which damage the rate of substrate enolization would not have such a preference. Given that k_2 (Scheme 2) for the wild-type equals 430 and 410 s^{-1} for substrates vermelone and DDBO, respectively, and that the two k_{cat}-distressed mutant enzymes (H110N and Y50F) have k_{cat} values equal to their k_2 values, then the relative k_2 values for DDBO versus vermelone [(k_2-(DDBO)/k_2(vermelone)] become 0.95, 6.2, and 0.68 for wild-type SD, H110N, and Y50F, respectively. These results are in accord with the H110N mutant lacking a strong hydrogen bond with the substrates' C3 hydroxyl in comparison to wild-type enzyme, thus welcoming the anomeric center provided by DDBO to assist in the elimination of hydroxide from substrates. In contrast, the Y50F mutation slows the reaction because it is less effective in protonating the substrates' carbonyl to assist enolization of the substrate, and accordingly, the anomeric carbon of DDBO does not help catalysis. In fact, vermelone is actually slightly preferred by Y50F over DDBO in terms of k_{cat}. Though these relative differences in k_{cat} (k_2) values are subtle, the two mutants seem to prefer substrates which help balance the transition state.

Summary of the Mechanism. The kinetic parameters for the mutant enzymes are consistent with a syn elimination of water from the substrates through an E1cb-like mechanism, and they help verify the importance of the individual side chains in supporting the elimination. We searched for experimental evidence implicating an enzyme-catalyzed enolization step within an E1cb-like mechanism by incubating SD with scytalone in D_2O versus time in an EIMS analysis and by incubating SD with ^{13}C-DHS in a NMR analysis and failed to find support for such a step being catalyzed by the enzyme. Large KIE's on k_2 and k_{cat}/K_m suggest that the kinetic barrier on the enzyme for the elimination of the C3 hydroxyl from scytalone is similar to that for enolization, likely accounting for our inability to detect an enol intermediate. The pH profile with substrate DDBO indicated a pK_a = 9.3 for k_{cat}/K_m which we attribute to an active-site residue having a role as a general acid. In the context of a syn elimination, this pK_a likely reports Y50; the phenol has a pK_a = 10−11 in water but would become more acidic when complexed with the active-site water molecule and the second tyrosine (Y30). That there is not a drop on the acidic side in the pH profile is understandable, as we could only measure kinetic parameters above pH 6.0. Due to its hydrophobic environment, H85 could easily have a pK_a below 6.0 and serve as the base in a syn elimination. Even though its basicity is raised by sharing a hydrogen bond with D31, H85 needs to approximate the pK_a of the Cα methylene in the transition state (*9*−*12*), and the acidity of this methylene is greatly enhanced by the enzyme through multiple interactions with the C1 carbonyl. Thus, enzymic side chains primarily involved in substrate recognition (S129 and N131), those primarily involved in assisting the enolization of substrate (Y30 and Y50 in conjunction with a water molecule), and one primarily involved in assisting the elimination of hydroxide from the substrates (H110) have been identified experimentally. It is likely that H85 (in complex with D31) has dual roles in assisting enolization and elimination of hydroxide from the substrates.

ACKNOWLEDGMENT

We thank Winnie Wagner for growing hundreds of grams of wild-type SD-producing cells of *E. coli*; Steve Hansen for synthetic work; Bruce Lockett for NMR spectroscopy; James Doughty and Robert Livingston for determinations of the protein masses by EIMS; and Alan Rendina and Ya-Jun Zheng for helpful discussions.

SUPPORTING INFORMATION AVAILABLE

The synthesis of **2** and **4** (Figure 3) and the preparation of site-directed mutants are detailed. One figure containing the nucleotide and corresponding amino acid sequence of SD is included (6 pages). This material is available free of charge via the Internet at http://pubs.acs.org.

REFERENCES

1. Bell, A. A., and Wheeler, M. H. (1986) *Annu. Rev. Phytopath. 24*, 411−451.
2. Howard, R. J., and Ferrari, M. A. (1989) *Exp. Mycol. 13*, 403−418.
3. Chumley, F. G., and Valent, B. (1990) *Mol. Plant-Microbe Interact. 3*, 135−143.
4. Ou, S. H. (1985) in *Rice Diseases*, 2nd ed., pp 109−201, C. A. B. International, Slough, U.K.
5. Lundqvist, T., Rice, J., Hodge, C. N., Basarab, G. S., Pierce, J., and Lindqvist, Y. (1994) *Structure (London) 2*, 937−944.
6. Andersson, A., Jordan, D. B., Schneider, G., and Lindqvist, Y. (1996) *Structure (London) 4*, 1161−1170.
7. Thompson, J. E., Basarab, G. S., Andersson, A., Lindqvist, Y., and Jordan, D. B. (1997) *Biochemistry 36*, 1852−1860.
8. Chen, J. M., Xu, S. L., Wawrzak, Z., Basarab, G. S., and Jordan, D. B. (1998) *Biochemistry 37*, 17735−17744.
9. Gerlt, J. A., Kozarich, J. W., Kenyon, G. L., and Gassman, P. G. (1991) *J. Am. Chem. Soc. 113*, 9667−9669.
10. Gerlt, J. A., and Gassman, P. G. (1992) *J. Am. Chem. Soc. 114*, 5928−5934.
11. Gerlt, J. A., and Gassman, P. G. (1993) *Biochemistry 32*, 11943−11952.
12. Anderson, V. E. (1998) in *Comprehensive Biological Catalysts*, Vol. 2, pp 115−133, Academic Press, New York.
13. Viviani, F., and Gaudry, M. (1990) *Tetrahedron 46*, 2827−2834.
14. Zheng, Y.-J., and Bruice, T. C. (1998) *Proc. Natl. Acad. Sci. U.S.A. 95*, 4158−4163.
15. Thompson, J. E., Basarab, G. S., Pierce, J., Hodge, C. N., and Jordan, D. B. (1998) *Anal. Biochem. 255, 256*, 1−6.
16. Cameron, D. W., and Sidell, M. D. (1976) *Aust. J. Chem. 29*, 1865−1867.
17. Viviani, F., Gaudry, M., and Marquet, A. (1992) *New J. Chem. 16*, 81−87.
18. Lundqivst, T., Weber, P. C., Hodge, C. N., Braswell, E. H., Rice, J., and Pierce, J. (1993) *J. Mol. Biol. 232*, 999−1002.
19. Andersson, A., Jordan, D., Schneider, G., Valent, B., and Lindqvist, Y. (1996) *Proteins: Struct., Funct., Genet. 24*, 525−527.
20. Sambrook, J., Fritsch E. F., and Maniatis, T. (1989). *Molecular Cloning. A Laboratory Manual*, 2nd ed., Cold Spring Harbor Laboratory Press, Cold Spring Harbor, New York.
21. Aiyar, A., and Leis, J. (1993) *BioTechniques 14*, 366−368.

22. Wawrzak, Z., Sandalova, T., Steffens, J. J., Basarab, G. S., Lundqvist, T., Lindqvist, Y., and Jordan, D. B. (1999) *Proteins: Struct., Funct., Genet.* (in press).
23. Thompson, J. E., and Jordan, D. B. (1998) *Anal. Biochem. 256*, 7−13.
24. Genetic Computer Group (1994) in *Program Manual for the Wisconsin Package, Version 8*, Genetic Computer Group, Madison, WI.
25. Bearne, S. L., and Wolfenden, R. (1995) *J. Am. Chem. Soc. 117*, 9588−9589.
26. Viviani, F., Gaudry, M., and Marquet, A. (1990) *J. Chem. Soc., Perkin Trans. 1 16*, 1255−1259.
27. Highet, R. J., and Chou, F. R. E. (1977) *J. Am. Chem. Soc. 99*, 3538−3539.
28. Tsai, H. F., Washburn, R. G., Chang, Y. C., and Kwon-Chung, K. J. (1997) *Mol. Microbiol. 26*, 175−183.
29. Zheng, L., Kennedy, M. C., Beinert, H., and Zalkin, H. (1992) *J. Biol. Chem. 267*, 7895−7903.

BI982952B